AKAP95 transports Cx43 into nucleus, regulating G1/S transition of A549 cells.

Zifeng Deng
State Key Laboratory of Molecular Vaccinology and Molecular Diagnostics, School of Public Health, Xiamen University

Rong Liu
State Key Laboratory of Molecular Vaccinology and Molecular Diganostics, School of Public Health, Xiamen University

Huiling Guo
State Key Laboratory of Molecular Vaccinology and Molecular Diagnostics, School of Public Health, Xiamen University

Luming Yao
State Key Laboratory of Celluar Stress Biology, School of Life Sciences, Xiamen University

FengKai Ruan
State Key Laboratory of Molecular Vaccinology and Molecular Diagnostics, School of Public Health, Xiamen University

Kai Wang
State Key Laboratory of Molecular Vaccinology and Molecular Diagnostics, School of Public Health, Xiamen University

Guihua Qiu
State Key Laboratory of Molecular Vaccinology and Molecular Diagnostics, School of Public Health, Xiamen University

Zhen Luo
State Key Laboratory of Molecular Vaccinology and Molecular Diagnostics, School of Public Health, Xiamen University

Guangping Luo
State Key Laboratory of Molecular Vaccinology and Mocular Diagnositcs, School of Public Health, Xiamen University

DongBei Guo
State Key Laboratory of Molecular Vaccinology and Molecular Diagnostics, School of Public Health, Xiamen University

Youliang Yao
State Key Laboratory of Molecular Vaccinology and Molecular Diagnostics, School of Public Health, Xiamen University

Yongxing Zhang (z63y94x@xmu.edu.cn)

State Key Laboratory of Molecular Vaccinology and Molecular Diagnostics, School of Public Health, Xiamen University https://orcid.org/0000-0002-0887-9713

Research

Keywords: Nuclear transport, AKAP95-Cx43 complex, cyclin D1, cyclin E1, TEM.

Posted Date: October 6th, 2020

DOI: https://doi.org/10.21203/rs.3.rs-85419/v1

Abstract

Purpose: Cx43 (connexin 43) has been found to inhibit cell cycle of tumor cells. No nuclear localization sequence of Cx43 was found but the protein has been found in nucleus. The process remains unclear. We are aiming at providing the model that AKAP95 (A-kinase anchoring protein) binds to and transports Cx43 into nucleus of lung cancer cells.

Methods: Lung cancer cells were arrested at preliminary stage (P), middle and late stage (M) of G1 phase and restriction point (R). Immunocoprecipitation (Co-IP) and Western blot (WB) were used to analyze expression and binding of AKAP95, Cx43, cyclin D1 and cyclin E1 at different stages of lung cancer cells during G1 phase. Confocal laser scanning microscopy (CLSM) was used to detect the location of proteins in arrested cells. Transmission electron microscope (TEM) with higher resolution was used to detect binding/aggregating and location of the above four proteins at subcellular level.

Results: 1) AKAP95 transports Cx43 into the nucleus through the nuclear pore mainly at R stage. Some AKAP95 and Cx43 form protein aggregates during the process. 2) Cyclin E1 was found to be bind/aggregate with AKAP95-Cx43 complex and involved in the nuclear transport of Cx43 mainly at R stage. 3)Cyclin D1 was found to bind with AKAP95 and Cx43 respectively but not to be involved in their aggregating and nuclear transport of Cx43.

Conclusions: 1) AKAP95 and Cx43 bind/aggregate to each other during G1 phase, forming AKAP95-Cx43 complexes/aggregates. After their binding/aggregating, AKAP95 targets nuclear pore and matrix, transporting Cx43 into nucleus. Formed AKAP95-Cx43 complexes/ aggregates do not dissociate in nucleus. The process can be summarized as ‘forming AKAP95-Cx43 complexes/aggregates; transporting Cx43 into nucleus; functioning remaining binding/aggregating’. 2) Cyclin D1 was only found to bind to AKAP95 and Cx43 respectively and function in cytoplasm while cyclin E1 was involved in the binding/aggregation of AKAP95 and Cx43, as well as the nuclear transport of Cx43.

Introduction

AKAP95 and Cx43 are vital factors that controls cell cycle, their aberrant expression always lead cancer [1–3]. In lung cancer, esophageal cancer etc. tissues, expression of AKAP95 increases while expression of Cx43 decreases [4–6]. AKAP95 mainly promotes cell proliferation by up-regulating cyclin Ds and cyclin Es while Cx43 down-regulates them to inhibit proliferation [7].

AKAP95 is the only protein that can target and enter nucleus of AKAPs family [8]. By binding to some proteins on nuclear membrane or in nuclear matrix, AKAP95 regulates transcription and promotes cell cycle etc. [9–14]. Recent studies have reported that a single cluster of basic amino acids (SV40-like class of nuclear localization signal) influences nuclear entry of AKAP95and p68RNA helicases is related to its ability to target the nuclear matrix [12,13]. AKAP95 also binds to nuclear pore complex protein to locate nuclear pores [14]. As a member of connexins family, Cx43 is a vital protein for gap junction communication of adjacent cells. Cx43 plays a variety of biological functions, including regulating

proliferation, development, and differentiation etc. of cells [2,15,16]. Our foregoing study had suggested that Cx43 might bind to AKAP95 [14] and regulate cell cycle by interacting with cyclin Ds and cyclin Es [5,7,17]. Unlike AKAP95, Cx43 does not have any nuclear localization sequence and cannot enter the nucleus autonomously [18]. However, Cx43 was found to bind to DNA in nucleus [19], which means some nuclear proteins may transport Cx43 into nucleus, and AKAP95 may be one of transporters.

Restriction point (RP) determines whether the cell is proliferating [20,21]. Cyclin D1 and cyclin E1 of cyclins family can enforce cells through RP, completing G1/S conversion [22,23]. Phosphorylation of retinoblastoma (Rb) relies on cyclin D-CDK4 and cyclin E1-CDK2, but cyclin D is relied earlier [14,26]. Activated cyclin D1 can promote the activation of cyclin E1/2-CDK2 [24,25], which is the vital regulators and effect target of E2Fs [26]. By promoting phosphorylation of Rb, cyclin E1/2 further promote the activation of E2Fs and G1/S conversion [22,25,26]. Non-phosphorylated Rb keeps binding to E2Fs, preventing DNA replication and transcription and leaving cells rest [20,21,23].

Results

AKAP95 bind to Cx43 and transfer it into nucleus during G1 phase in A549 cells.

Treated with Lovastatin, Mimosine and Thymidine respectively, cells were arrested at P, M and R stages [27–30]. Flow cytometry (FCM) was used to detect the cell cycle (Fig. 1A). After treated with Lovastatin and Mimosine respectively, proportion of cells in G1 phase increased while proportion of cells in G2 phase decreased. No significant changes were found of percentage of cells in S phase compared with the control group. Percentage of cells in G1 phase of Lovastatin group was higher than Mimosine group. In Thymidine group, whose cells were mainly arrested between late G1 and early S phase, proportion of cells in S phase increased while proportion of cells in G1 phase decreased. No significant change was found of percentage of cells in G2 phase compared with the control group (Fig. 1Aa). Figure 1.Ab shows the bar chart of the statistical results of Fig. 1Aa. These data show that cells were arrested in P, M, and R stage efficiently.

We further detected expression of AKAP95 and Cx43 in cancer and normal lung cells at different stages of G1 phase (Fig. 1B). In A549 cells, both AKAP95 and Cx43 had low level expression during P and M stages but highly expressed in R stage (Fig. 1Ba). Expressions of both AKAP95 and Cx43 in these three stages were significant respectively ($p < 0.05$), and both of their expression increased gradually form P to R stage and peaked at R stage. In Beas-2B cells, AKAP95 expressed much lower than that in A549 cells or Cx43 in Bease-2B cells (Fig. 1Bb). Both AKAP95 and Cx43 in Beas-2B cells highly expressed form M stage, which was earlier than that in A549 cells, and kept highly expression.

Since the expression of AKAP95 and Cx43 in G1 phase showed a consistent increasing trend, we detected the localization of these two proteins in different stages by CLSM. The blue fluorescence showed DNA of nucleus and green and red fluorescence showed AKAP95 and Cx43 respectively. In our images, AKAP95 mainly expressed in nucleus during G1 phase (Fig. 2Ab,h,n). In addition, some strong fluorescent patches could be found in nucleus, suggesting that some AKAP95 aggregated and form protein aggregates. Cx43

expressed both in nucleus and cytoplasm during G1 phase (Fig. 2Ac,i,o). Due to superposition of blue and red fluorescence, purple color could be observed in Merge images of DAPI and Cx43 (Fig. 2Ae, k, q) and yellow color could be observed in Merge images of AKAP95 and Cx43 (Fig. 2Af, l, r), suggesting that some Cx43 might bind to DNA and AKAP95 in nucleus.

By TEM assay, we further confirmed that AKAP95 could bind to Cx43 both in cytoplasm and nucleus and could transport it into nucleus through nuclear pore. In Fig. 2Ba, green triangle pointed to AKAP95 (15 nm label) and red triangle pointed to Cx43 (10 nm label). Taking the scale on the picture as the standard, the distance of the two labels was less than 15 nm, suggesting that AKAP95 can bind to Cx43 in cytoplasm (It is generally considered that two proteins bind to each other when the distance of gold labels of them is less than 15 nm in TEM images [31,32]). Figure 2Bb showed that AKAP95-Cx43 complex just entered nucleus through nuclear pore. Blue arrow refers to the nuclear membrane. The nuclear pore is between the two arrows on the right of the image (the interval marked by the red line).

Dynamic process of nuclear transport of Cx43.

We had further detected the process of nuclear transport of Cx43 in cells arrested at different stages of G1 phase by TEM assay.

In TEM assay, different concentrations of gold labeled IgG may affect the results. When the dilution ratio of Gold labeled IgG was 1:100, a few gold particles showed nonspecific adhesion causing false positive while when the dilution ratio was 1:100, though false positive could be avoided, some target proteins could not be labeled and displayed caused by low concentration of gold labeled IgG. In order to verify whether there was false positive interference under our experimental conditions, Rabbit anti- and Mouse anti-GAPDH were used to incubated sections before incubation with Gold labeled IgG (15 nm and 10 nm) in Positive Control while PB buffer was used instead of specific GAPDH antibodies in Negative Control group. Results showed that single gold labels could be found in Positive control (Fig. 3Aa) and distance of different labels was significantly more than 15 nm (Fig. 3Ab). Scales on each TEM images were chosen to be standard and distance of 10 pairs of 15 nm and 10 nm gold labels in each group were detected. Average distance of different gold labels of Control (Positive Control) group was more than 100 nm and no nonspecific aggregation had been detected while it was less than 10 nm in arrested cells groups, suggesting that our positive results were reliable. Only extremely few gold labels were found in Negative Control groups, and no nonspecific aggregation were found (Fig. 3B), suggesting that the false positive interference could be ignored under our experimental condition.

In arrested A549 cells, we found that binding of AKAP95 and Cx43 could be detected during whole G1 phase and binding of the them could be detected in nucleus at three stages of G1 phase (Fig. 4A). Interestingly, we found that AKAP95 could bind to Cx43 in two forms. In addition to bind to each other and form AKAP95-Cx43 complexes, we had detected aggregations of gold labels with different diameters, suggesting that some AKAP95 and Cx43 proteins could aggregate and form bigger protein aggregates. AKAP95-Cx43 complexes/aggregates existed in both nucleus and cytoplasm, suggesting that both the complexed and aggregates of AKAP95 and Cx43 had the ability of entering nucleus. In nucleus, no single

AKAP95 nor Cx43 was found, suggesting that Cx43 kept binding to AKAP95 after transported into nucleus. In Beas-2B cells, we had found AKAP95-Cx43 complexes/aggregates both in nucleus and cytoplasm as well (Fig. 4B). However, owing to expression level of AKAP95 was lower than that of Cx43 in Beas-2B cells, we had found some single 10 nm gold labels (Cx43) which could not enter the nucleus, suggesting that Cx43 could not enter the nucleus without transport of AKAP95.

To clarify the process of nuclear transport of Cx43, we further photographed more TEM images of various locations of AKAP94-Cx43 complexes/aggregates in A549 cells at different stages of G1 phase and organized a series of typical images that could represent every stages of the process (Fig. 5). After expression, AKAP95 could bind to Cx43 in cytoplasm and form AKAP95-Cx43 complex, and some AKAP95 and Cx43 could form aggregates as well during the stage (Fig. 5a). In formed AKAP95-Cx43 complex/aggregates, AKAP95 then targeted nuclear membrane, driving the complex/aggregates to move towards the nuclear membrane (Fig. 5b). After located on the nuclear membrane (Fig. 5c), AKAP95 further targeted nuclear matrix and transported Cx43 into nucleus (Fig. 5d). In nucleus, AKAP95 and Cx43 kept binding and further functioned in the form of AKAP95-Cx43 complex/aggregates (Fig. 5e, f).

Cyclin E1 was involved in nuclear transport of Cx43 during G1 phase.

AKAP95 and Cx43 could bind to cyclin D1 and competitively bind to cyclin E1/E2 respectively, regulating the G1/S conversion [7,33–35]. Our previous study had shown that cyclin D1 and cyclin E1 were correlated with AKAP95 respectively while were not correlated with Cx43 [34]. To further discuss if cyclin D1 and cyclin E1, which were important regulators of G1/S transition, were involved in nuclear transport process of Cx43, we analyzed these proteins in arrested A549 cells.

Our results showed that cyclin D1 highly expressed at P and S stages while lowly expressed at R stage (Fig. 6Aa, the third row). Expressions of cyclin E1 were low at P and M stages while peaked at R stage (Fig. 5Aa, the fourth row). Statistical results were shown in Fig. 6Ab. According to the data, expression of cyclin E1 during G1 phase changed similarly to that of AKAP95 and Cx43 while cyclin D1 showed the opposite trend (Fig. 5Ab). Specific AKAP95 and Cx43 antibodies were used in Co-IP assay to detect protein bindings in arrested cells. Both cyclin D1 and cyclin E1 could be detected in coprecipitation in Co-IP: AKAP95 group (Fig. 5B), suggesting that AKAP95 could bind to cyclin D1 and cyclin E1 during whole G1 phase. Similar results were found in Co-IP: Cx43 group (Fig. 5C), suggesting that Cx43 could bind to cyclin D1 and cyclin E1 during G1 phase as well. These results suggested that AKAP95, Cx43, cyclin D1, and cyclin E1 could bind to each other and formed at least four complexes, including AKAP95-cyclin D1, AKAP95-cyclin E1, Cx43-cyclin D1, and Cx43-cyclin E1 during G1 phase. However, owing to the difference of expression level of the four proteins, we considered that AKAP95-cyclin D1 and Cx43-cyclin D1 mainly existed at P and M stage while AKAP95-cyclin E1 and Cx43-cyclin E1 were formed mainly at R stage of G1 phase.

In CLSM images, no significant nuclear expression of cyclin D1 was found during whole G1 phase (Fig. 7A). Cyclin E1 mainly expressed at R stage and obvious nuclear expression could be detected at this stage. In addition, strong fluorescent plaques of cyclin E1, similar with AKAP95, could be found in cells at

R stage. During the other two stages, cyclin E1 mainly located in cytoplasm (Fig. 7B). These images suggested that even both cyclin D1 and cyclin E1 could bind to AKAP95 and Cx43 respectively, cyclin E1 might take participate in nuclear transport of Cx43 while cyclin D1 not.

We further carried out TEM assay to seek direct evidences at subcellular level. Results showed that gold labels that marked cyclin D1 only existed in cytoplasm. Some cyclin D1 could located on nuclear membrane, but could not enter nucleus (Fig. 7C), suggesting that cyclin D1 did not entered nucleus with AKAP95 and might dissociate from AKAP95 before it entered the nucleus at the latest. On the contrary, cyclin E1 could be detected both in nucleus and cytoplasm in P, M, and R stage cells. Significant aggregations of gold labels could also be found, especially in R stage cells (Fig. 7D), suggesting that cyclin E1 entered nucleus with AKAP95 mainly at R stage and might be involved in aggregations of AKAP95 and Cx43.

When AKAP95 and cyclin D1 were simultaneously labeled in cells, AKAP95-cyclin D1 complexes located in cytoplasm during whole G1 phase. Single 10 nm gold labels (AKAP95) could be found in nucleus while 15 nm labels (cyclin D1) could not. In addition, no significant protein aggregation was found (Fig. 8Aa,b,c). Images of Cx43/cyclin D1 group were similar and no labels of cyclin D1 were found in nucleus (Fig. 8Ad,e,f). In R stage cells, we didn't find Cx43-cyclin D1 complex this time. We considered that highly expressed Cx43 might promotes degradation cyclin D1, which lowly expressed at R stage, after their binding, thus we didn't catch some images. It was completely different when cyclin E1 was labeled together with AKAP95 and Cx43 respectively. Both AKAP-cyclin E1 complexes and Cx43-cyclin E1 complexes could entered nucleus and protein aggregation could be found during G1 phase (Fig. 8B). These results had supported our conjecture that cyclin E1 was involved in aggregations of AKAP95 and Cx43 while cyclin D1 was not.

Discussion

Our previous pointed out that AKAP95 only bound to Cx43 at late G1 phase [1]. However, AKAP95-Cx43 complex was also detected at early and middle stages of G1 phase by TEM assay this time. We considered that owing to low expression of AKAP95 and Cx43 at early and middle stages of G1 phase, compared with situation at late G1 phase, binding of the two protein could hardly be detected by Co-IP/WB assay while the problem could be solved by TEM which had higher resolution.

Though AKAP95 and Cx43 expressed and bound to each other from early G1 phase, they mainly formed complexes/aggregates near RP (from late G1 phase to early S phase). After bound to AKAP95, Cx43 could be transported into nucleus. They would not dissociate in nucleus and Cx43 might bind to DNA and further functioned in the forms of AKAP95-Cx43 complex or aggregate. Still, nuclear transport of Cx43 happened during whole G1 phase but mainly at R stage.

Here, we conclude the process of nuclear transport of Cx43 as :1) AKAP95 bound to Cx43, forming AKAP95-Cx43 complexes or aggregates in cytoplasm. 2) AKAP95 targeted the nuclear membrane, guiding AKAP95-Cx43 complexes/aggregates move towards the nuclear membrane and located on it. 3)

AKAP95 continued to target nuclear matrix, transporting Cx43 into nucleus through nuclear pore in forms of AKAP95-Cx43 complexes/aggregates. Cx43 kept binding to AKAP95 and further functioned in forms of AKAP95-Cx43 complexes/aggregates in nucleus. The transport process could happen from P stage, but Cx43 was transported into nucleus mainly at R stage when both AKAP95 and Cx43 highly expressed.

AKAP95 and Cx43 regulated cell cycle mainly by interacting with cyclin Ds and cyclin Es during G1 phase [7,17,22,23]. During G1 phase, AKAP95 could up-regulate expression of cyclin D1 and further cyclin E1 and promoting cell cycle while Cx43 opposite affected cell cycle by accelerating degradation of cyclin D1 and cyclin E1 [7,14]. Though both cyclin D1 and cyclin E1 finally promoted phosphorylation of Rb [22,23], they played different roles in nuclear transport process of Cx43.

Cyclin D1 highly expressed at P and M stage. AKAP95 and Cx43 could bind to it respectively and regulate its expression level. AKAP95 up-regulated expression of cyclin D1, which could further promote activation of cyclin E1 and inhibit the inhibitory effect of p21 and p27 on cyclin E-DCK2 activity by binding to it while Cx43 promoting its degradation [7,36]. We found that both AKAP95-cyclin D1 and Cx43 cyclin D1 located only in cytoplasm at these two stages, suggesting that cyclin D1 might mainly interacted with AKAP95 and Cx43 and influenced cyclin E1 in cytoplasm, promoting Rb phosphorylation and G1/S transition indirectly by cyclin E1.

At R stage, cyclin E1 highly expressed and promoted the G1/S conversion by promoting hypo- and hyper-phosphorylation of Rb [18]. AKAP95 and Cx43, which highly expressed at R stage as well, could competitively bind to cyclin E1 and regulated its expression and further phosphorylation of Rb [7]. On the one hand, AKAP95 and Cx43 bound to cyclin E1 up/down-regulating its expression respectively, and on the other hand, AKAP95 and Cx43 inhibiting each other's binding and effect on cyclin E1 by forming AKAP95-Cx43 complexes. Owing to difference of expression level of AKAP95 and Cx43 in lung cancer cells and normal lung cells, effect of the protein which relatively expressed higher mainly showed out. Moreover, though Fig. 8 suggesting that both AKAP95-cyclin E1 and Cx43-cyclin E1 might existed in nucleus, we considered that owing to Cx43 could accelerate degradation of cyclin E1, Cx43-cyclin E1 might not actually existed in nucleus. Because no AKAP95 were labeled and showed, in fact, aggregates of gold labels in Fig. 8Bd., e., and f. might be AKAP95-Cx43 and AKAP95-cyclin E1 aggregates. Interestingly, significant aggregates were found in images of cyclin E1 and AKAP95/Cx43 groups while not in cyclin D1 groups. We consider that cyclin E1 was involved in protein aggregation of AKAP95 and Cx43 and nuclear transport of Cx43. In addition, we didn't find dissociation of AKAP95/Cx43 and cyclin E1 after complexes/aggregates of them formed, thus we considered that AKAP95 and Cx43 might directly affect cyclin E1 and entered nucleus together with cyclin E1 by binding to it rather than by interacting with other proteins. However, significance of aggregation of these proteins remained unclear and we need carried out further work to clarify it.

Together with our foregoing data [5,7,17], we concluded the participation of cyclin E1 in nuclear transport of Cx43 as:1) AKAP95, Cx43 and cyclin E1 bound to each other and formed AKAP95-Cx43, AKAP95-cyclin E1, Cx43-cyclin E1 complexes/aggregates. Owing to function of Cx43, cyclin E1 that bound to Cx43 were

finally degraded. 2) Aggregates of AKAP95-Cx43 and AKAP95-cyclin E1 were drove to nucleus and transported into nucleus. 3) Cyclin E1 in nucleus kept binding to AKAP95, promoting phosphorylation of Rb and G1/S transition.

Conclusion

Our article had provided nuclear transport model of Cx43 and discussed the specific processes.

Moreover, we had investigated cyclin E1's participation in process of nuclear transport of Cx43 and discussed the process of cyclin E1 promoting G1/S transition.

Materials And Methods

Antibodies

Mouse anti-AKAP95(sc-100643), anti-Cx43(sc-13558), anti-cyclin D2(sc-53637), anti-cyclin D3(sc-6283), anti-cyclin E2 (sc-28351) were purchased from Santa Cruz (Texas, USA); Mouse anti-Cx43(ab79010), Rabbit anti-AKAP8(ab134923), anti-Cx43(ab235586), anti-cyclin D1(ab134175), anti-cyclin D2(ab207604), anti-cyclin D3(ab28283), anti-cyclin E1(ab33911), anti-cyclin E2(ab40890) were purchased from Abcam(Cambridge, UK); Mouse anti GADPH(T0004), Rabbit anti-AKAP8(AF0333), anti-Cx43(AF0137), anti-GADPH(AF7021) were purchased from Affnity Biosciences(Ohio, USA);Goat Anti-rabbit IgG/Gold (AB-0295G-Gold, 15 nm), Goat Anti-mouse IgG/Gold (AB-0296R-Gold, 10 nm) were purchased from Leading Biology Inc. (California, USA);Goat Anti-rabbit IgG FITC(HA1004), Goat Anti-mouse IgG H&L TRITC(HA1017) were purchased from Hangzhou HuaAn Biotechnology Co., Ltd (Hangzhou, China).

Reagents

Protein A/G Plus-Agarose(sc-2003) were purchased from Santa Cruz(Texas, USA);Lovastatin, Mimosine, DAPI, Antifade Solution and Cell Cycle and Apoptosis Analysis Kit were purchased from Dalian Meilun Biotechnology Co., Ltd (Dalian, China); Thymidine was purchased from Solarbio(Beijing, China); Western Lab Peroxidase (E1050) were purchased from Beijing LABLEAD BIOTECH (Beijing, China).

Cell Culture And Protein Extraction

A549 and Beas-2B cells culture: A549 and Beas-2B cells lines were preserved in our laboratory. Cells were cultured in DMEM medium (containing 10% fetal bovine serum) under the conditions of 5% CO2, 90% humidity ,37°C. Lovastatin (0.015 μmol/mL), Mimosine(0.004 μmol/mL,and Thymidine0.003 μmol/mL was added into the medium and cultured for 24 h when cells needed to be arrested. Total proteins were extracted using RIPA/p0013 buffer from synchronous cells.

Co-immunoprecipapation

Add 5 μg primary antibody to every 500 μg total protein. After incubated by a shaker at 4℃ overnight(8 h), add 20 μl Protein A/G plus-agarose and keep incubation for another 8 hours. Collect the supernatant after centrifugation (3000 rpm), then wash the coprecipitate 2–3 times by PBS buffer. Lysate (RIPA/p0013 buffer) was used to resuspend and dissolve coprecipitate. The protein (coprecipitate and supernatant) can be detected or stored at -20℃ after boiled. Add Loading buffer to protein before boiling.

Western Blot

Add 50 μg protein sample to per lane of SDS-PAGE gel. Electrophoresis was performed under 120 V constant pressure and protein was transferred on PVDF membranes at a constant current of 300 mA. Membranes were incubated with specific primary antibodies (1:3000) overnight (8 h) at 4℃ after incubated with skimmed milk powder for 1 h. Membranes were then incubated with IgG antibodies at 37℃ for 1 hour. Proteins were detected by BIO RAD Chemi DOC XRS + Imaging System and bands of proteins were analyzed using Image Lab. Bands of GAPDH or Input group were used to normalize the date of other groups. Each experiment was repeated three time.

Statistical analysis

IBM SPSS Statistics 20(SPSS Inc., Chicago, IL, USA) was used to analyze statistics. Data was compared using independent t- test and α<0.05 was considered significant. Statistical charts were exported by GraphPad Prism8.

Flow Cytometry

Cells were collected by centrifugation (3000 rpm) and fixed with 75% ethanol at 4℃ for 18–24 hours. Cell cycle detection kit was used to stain cells and stained cells should be washed using PBS buffer 1–2 times before detection using flow cytometry (Beckman CytoFLEX). FlowJo V10 was used to analyze data.

Immunofluorescence

Slides were taken out when cell density reach 60%-80%. Slides were fixed with 4% paraformaldehyde for 1 hour and incubated with 1% BSA for 30 minutes. Under the 4℃ condition, slides were incubated with specific primary antibodies overnight (8 h) before incubated with fluorescent IgG antibodies for 1 hour at 37℃. After stain cells with DAPI and add quenching agent to slides, confocal laser scanning microscopy (Olympus FV1200) was used to observe cells. Images were analyzed by FV10-ASW 4.2 Viewer.

Immunoelectron Microscopy

Centrifuge(3000 rpm) and collect cells, and then fix cells with 4% paraformaldehyde for 2–3 hours at 4℃. After washed by PB buffer (0.0162M Na_2HPO_3 + 0.038M NaH_2PO_3) for 3 times, gradient concentration of ethanol was used in the dehydration of cells. Cells were embedded by LR White resin and were sliced after that. The slides were sealed by 1% BSA for 15–20 minutes at room temperature and incubated with specific primary antibodies overnight (8 hours) at 4℃. PB buffer was used to wash slides for 3 times (5 minutes for each time), and after that, under 37℃ condition, slides were incubated with

Gold labeled IgG antibodies for 1 hour at 37℃. Wash slides for 3 times (5 minutes for each time). Slides then had been fixed by 2.5% glutaraldehyde and washed by PB buffer for 3 times (3 minutes for each time). After stained with uranium and lead, slides were detected and photographed by transmission electron microscope (Tecnai G2 Spirit BioTwin).

List Of Abbreviations

A-kinase anchoring protein (AKAP95); Connexin 43 (Cx43); Preliminary stage of G1 phase (P); Middle stage of G1 phase (M); Restriction point (R); Western blot (WB); Confocal laser scanning microscopy (CLSM); Transmission electron microscope (TEM); Flow cytometry (FCM).

Declarations

Ethics approval and consent to participate

Not applicable.

Consent for publication

All authors agree to publish the article.

Availability of data and material

Data available.

Competing interests

No inflect of interests of this article.

Funding

This research was funded by National Natural Science Foundation of China (No.81071927& No.31741006), the Natural Science Foundation of Fujian Province of China (No. 2016J01407), XMU Training Program of Innovation and Entrepreneurship for Undergraduates (No.20720192016), Innovation Practice Platform for Undergraduates Students, School of Public Health Xiamen University (No.202004&No.202005).

Authors' contributions

ZD and YZ contributed to study design; ZD and RL were the main operators; HG, LY and FR provided methodological help; KW, GQ, ZL and GL helped with the software; DG and YL provided some equipment support; ZD wrote the article and YZ revised the article.

Acknowledgements

Dr. Qingbing Zheng and Mr. Chaoqing Wu had helped to finish the article.

References

1. Decrock E, De Vuyst E, Vinken M et al. Connexin 43 hemichannels contribute to the propagation of apoptotic cell death in a rat C6 glioma cell model. Cell Death Differ. 2009,16(1):151-163.
2. Lezcano V, Bellido T, Plotkin LI et al. Role of connexin 43 in the mechanism of action of alendronate: Dissociation of anti-apoptotic and proliferative signaling pathways. Archives of Biochemistry and Biophysics. 2012,518(2):95-102.
3. Johnstone SR, Best AK, Wright CSet al. Enhanced connexin 43 expression delays intra-mitoitc duration and cell cycle traverse independently of gap junction channel function. Cell Biochem. 2010,110(3):772-782.
4. Wenzhi Liu, Suhang Hua, Yue Dai et al. Roles of Cx43 and AKAP95 in ovarian cancer tissues in G1/S phase. Int J Clin Exp Pathol. 2015,8(11):14315–14324.
5. ShuoWang, KaiWang, Zifeng Deng et al. Correlation between the protein expression levels of A-kinase anchor protein95, p-retinoblastoma (Ser780), cyclin D2/3, and cyclin E2 in esophageal cancer tissues. Asia-Pac J Clin Oncol. 2019,1–5.
6. Zhiyu Guan, Winxin Zhuang, Hui Lei et al. Epac1, PDE4, and PKC protein expression and their correlation with AKAP95 and Cx43 in esophagus cancer tissues. Thoracic Cancer. 2017,8:572–576.
7. Renzhen Chen, Yu Chen, Yangyang Yuan et al. Cx43 and AKAP95 regulate G1/S conversion by competitively binding to cyclin E1/E2 in lung cancer cells. Thoracic Cancer. 2020,11:1594–1602
8. Jing Hu, Alireza Khodadadi-Jamayran, Miaowei Mao et al. AKAP95 regulates splicing through scaffolding RNAs and RNA processing factors. Nat Commun. 2016,7:13347.
9. Wong, W. and Scott, J. D. AKAP signalling complexes: focal points in space and time. Nat. Mol. Cell Biol. 2004,5:959–970.
10. Yun Li, Gary D Kao, Benjamin A Garcia et al. A novel histone deacetylase pathway regulates mitosis by modulating Aurora B kinase activity. Genes Dev. 2006,20:2566–2579.
11. Jungmann, R. A. and Kiryukhina, O. Cyclic AMP and AKAP-mediated targeting of protein kinase A regulates lactate dehydrogenase subunit A mRNA stability. J. Biol. Chem. 2005,280:25170–25177.
12. L Akileswaran, J W Taraska, J A Sayer et al. A-kinase-anchoring Protein AKAP95 Is Targeted to the Nuclear Matrix and Associates With p68 RNA Helicase. J Biol Chem 2001,276 (20):17448-17454.
13. Hicks G. R., Raikhel N.V. Protein Import Into the Nucleus: An Integrated View. Annu. Rev. Cell Dev. Biol. 1995,11:155–188.
14. Graciela López-Soop, Torunn Rønningen, Agnieszka Rogala et al. AKAP95 interacts with nucleoporin TPR in mitosis and is important for the spindle assembly checkpoint. Cell Cycle 2017,16 (10):947-956.
15. Decrock E, De Vuyst E, Vinken M et al. Connexin 43 hemichannels contribute to the propagation of apoptotic cell death in a rat C6 glioma cell model. Cell Death Differ. 2009,16(1):151-163.

16. Bruzzone R. Learning the language of cel-cell communication through connexin channels. Genome Biol. 2001,2(11): 4027.1-4027.5.
17. Xiangyu Kong, Dengcheng Zhang, Wenxin Zhuang et al. AKAP95 promotes cell cycle progression via interactions with cyclin E and low molecular weight cyclin E. Am J Transl Res. 2016,8(2):811-826.
18. Dang X., Doble B. W. and Kardami E. The carboxy-tail of connexin-43 localizes to the nucleus and inhibits cell growth. Molecular and Cellular Biochemistry. 2003,242:35–38.
19. Xiaoxuan Chen, Xiangyu Kong, Wenxin Zhuang et al. Dynamic changes in protein interaction between AKAP95 and Cx43 during cell cycle progression of A549 cells. Sci Rep. 2016, 6:21224.
20. Riaan Conradie, Frank J. Bruggeman, Andrea Ciliberto et al. Restriction point control of the mammalian cell cycle via the cyclin E/Cdk2: p27 complex. FEBS Journal 2010,277: 357–367.
21. Planas-Silva MD and Weinberg RA. The restriction point and control of cell proliferation. Current Opin. Cell Biol. 1997, 9:768–772.
22. Johannes Boonstra. Progression Through the G1-Phase of the On-Going Cell Cycle. Journal of Cellular Biochemistry. 2003,90:244–252.
23. Irina Neganova and Majlinda Lako. G1 to S phase cell cycle transition in somatic and embryonic stem cells. Journal of Anatomy. 2008,213:30-44.
24. Ignacio Perez-Roger, Soo-Hyun Kim, Beatrice Griffiths et al. Cyclins D1 and D2 mediate Myc-induced proliferation via sequestration of $p27^{Kip1}$ and $p21^{Cip1}$. The EMBO Journal. 1999,18 (19) :5310–5320.
25. Ylva HEDBERG, Estela DAVOODI, Bo¨rje LJUNGBERG et al. Cyclin E and P27 protein content in human renal cell carcinoma: clinical outcome and associations with cyclin D. Int. J. Cancer. 2002,102:601–607.
26. Rory Donnellan and Runjan Chetty. Cyclin E in human cancers. The FASEB Journal. 1999,13:773-780.
27. JAN LAMPRECHT, CEZARY WÓJCIK, MAREK JAKÓBISIAK et al. Lovastatin induces mitotic abnormalities in various cell lines. Cell Biology International. 1999,23(1):51–60.
28. Paul A. Watson, Hartmut H. Hanauske-Abel, Alan Flint et al. Mimosine Reversibly Arrests Cell Cycle Progression at the G1-S Phase Border. Cytometry. 1991,12:242-246.
29. Lalande M. A reversible arrest point in the late G1 phase of the mammalian cell cycle. Exp Cell Res.1990,186:332-339.
30. Cooper, K. Z. Chen and S. Ravi. Thymidine block does not synchronize L1210 mouse leukaemic cells: implications for cell cycle control, cell cycle analysis and whole-culture synchronization. Cell Prolif. 2008,41:156-167.
31. Scott R. Johnstone, Brett M. Kroncke, Adam C. Straub et al. MAPK Phosphorylation of Connexin 43 Promotes Binding of Cyclin E and Smooth Muscle Cell Proliferation. Circ Res. 2012,111:201-211.
32. Neetu M. Gulati, Udana Torian, and John R. Gallagher et al. Immunoelectron Microscopy of Viral Antigens. Current Protocols in Microbiology. 2019,53-86.
33. Arsenijevic T, Degraef C, Dumont JE et al. A novel partner for D-type cyclins: protein kinase A-anchoring protein AKAP95. Biochemical Journal. 2004,378(2):673-679.

34. Zhao S, Yi M, Yuan Y, et al. Expression of AKAP95, Cx43, cyclinE1 and cyclinD1 in esophageal cancer and their association with the clinical and pathological parameters. International Journal of Clinical and Experimental Medicine. 2015,8(5):7324-7332.
35. Matsushime H, Quelle DE, Shurtleff SA et al. D-type cyclin-dependent kinase activity in mammalian cells. Mol Cell Biol. 1994,14(3):2066-2076.
36. Dean Smith, David Mann and Kwee Yong. Cyclin D type does not influence cell cycle response to DNA damage caused by ionizing radiation in multiple myeloma tumours. British Journal of Haematology. 2016,173:693–704.

Figures

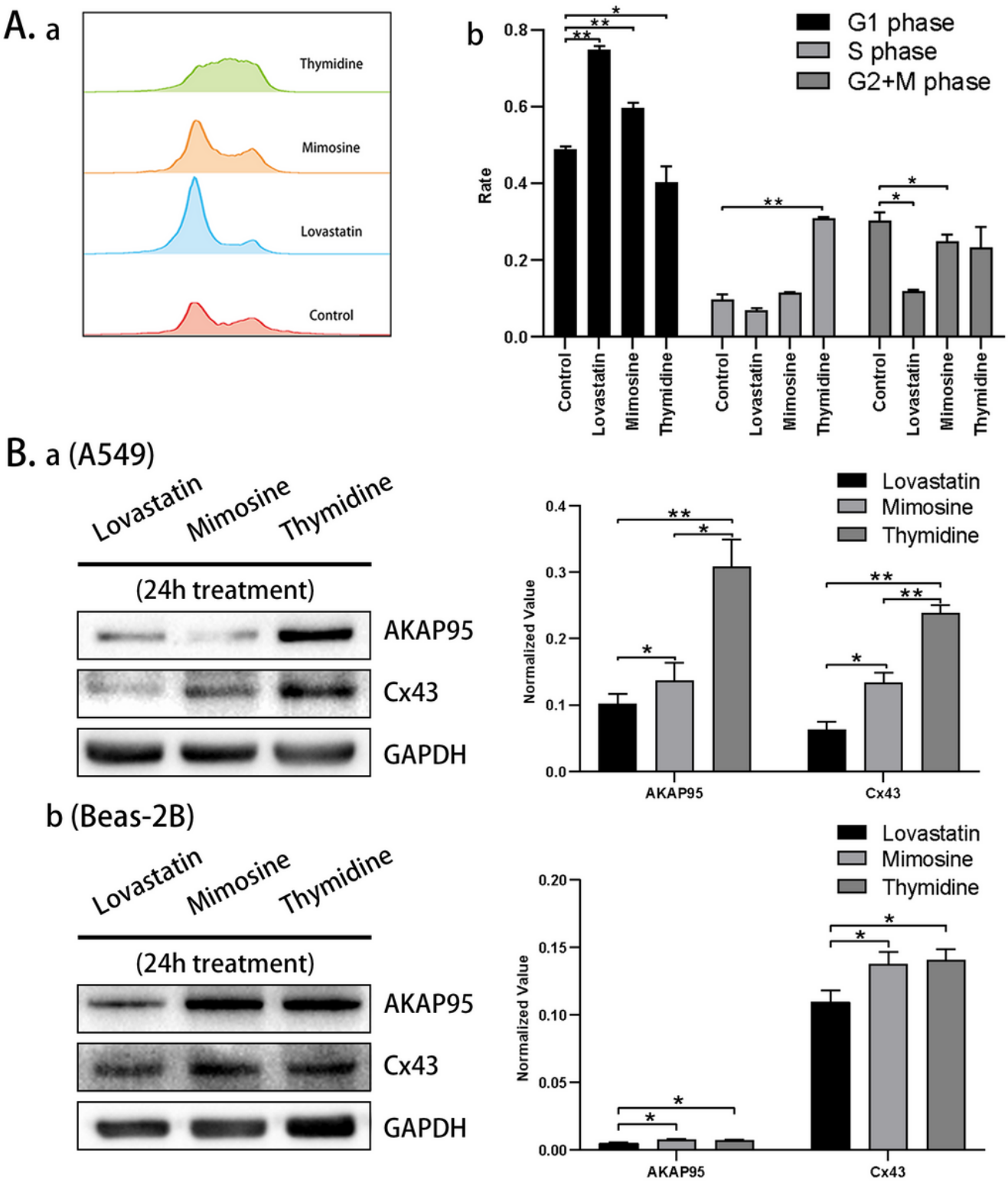

Figure 1

Expression of AKAP95 and Cx43 in arrested cells. (A) FCM was used to detect phases of arrested A549 cells. Cells of control group were treated without drugs. (B)Total proteins were extracted from arrested A549 and Beas-2B cells and detected by WB. Gray value of GAPDH band was used to normalized data. The ratio of gray value of AKAP95 and Cx43 band to GAPDH band was used as variable for statistical analysis among groups (* means $p<0.05$; **means $p<0.01$).

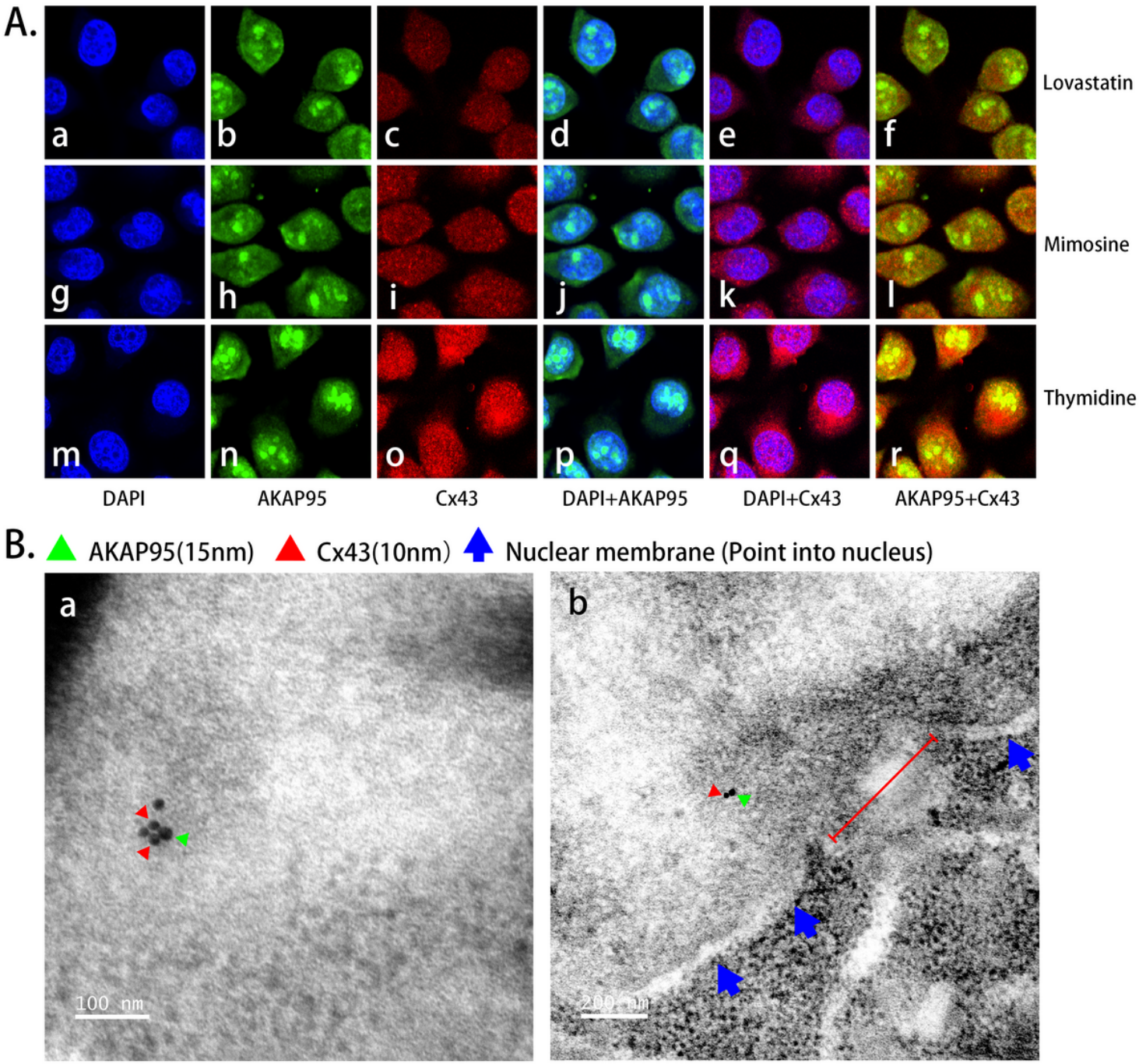

Figure 2

Expression of AKAP95 and Cx43 in arrested cells. (A) FCM was used to detect phases of arrested A549 cells. Cells of control group were treated without drugs. (B)Total proteins were extracted from arrested A549 and Beas-2B cells and detected by WB. Gray value of GAPDH band was used to normalized data. The ratio of gray value of AKAP95 and Cx43 band to GAPDH band was used as variable for statistical analysis among groups (* means $p<0.05$; **means $p<0.01$).

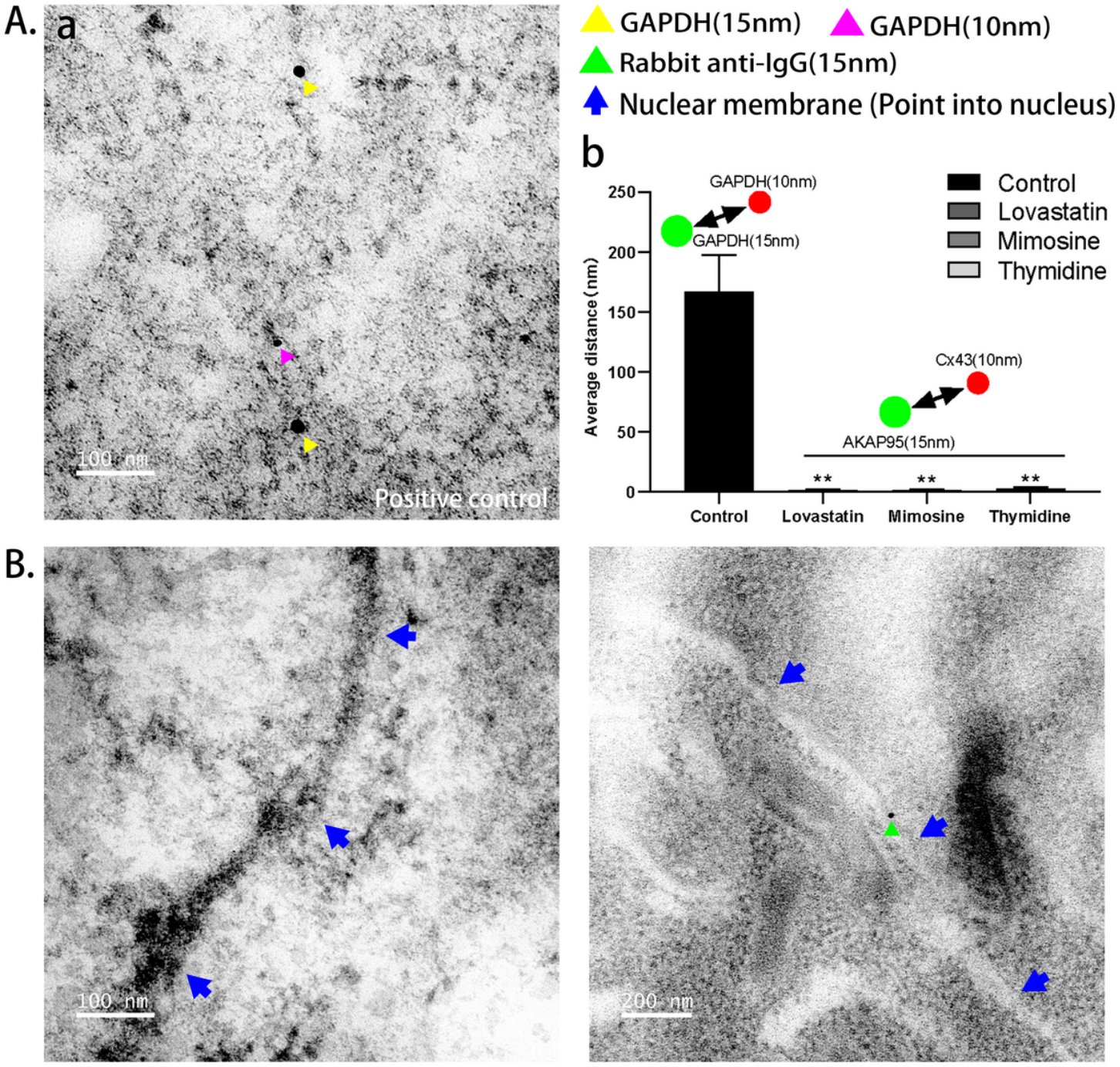

Figure 3

Expression of AKAP95 and Cx43 in arrested cells. (A) FCM was used to detect phases of arrested A549 cells. Cells of control group were treated without drugs. (B)Total proteins were extracted from arrested A549 and Beas-2B cells and detected by WB. Gray value of GAPDH band was used to normalized data. The ratio of gray value of AKAP95 and Cx43 band to GAPDH band was used as variable for statistical analysis among groups (* means $p<0.05$; **means $p<0.01$).

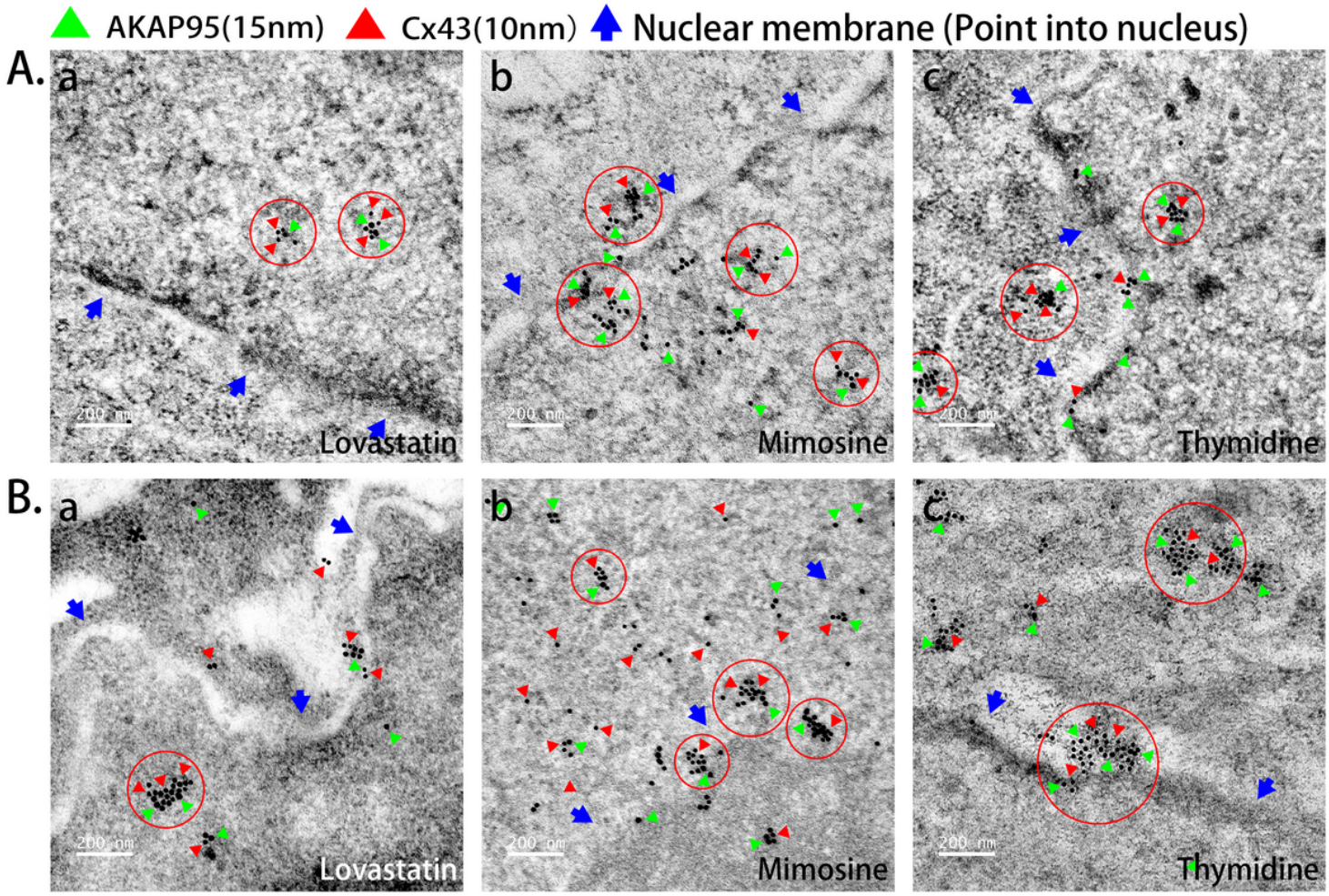

Figure 4

Expression of AKAP95 and Cx43 in arrested cells. (A) FCM was used to detect phases of arrested A549 cells. Cells of control group were treated without drugs. (B)Total proteins were extracted from arrested A549 and Beas-2B cells and detected by WB. Gray value of GAPDH band was used to normalized data. The ratio of gray value of AKAP95 and Cx43 band to GAPDH band was used as variable for statistical analysis among groups (* means $p<0.05$; **means $p<0.01$).

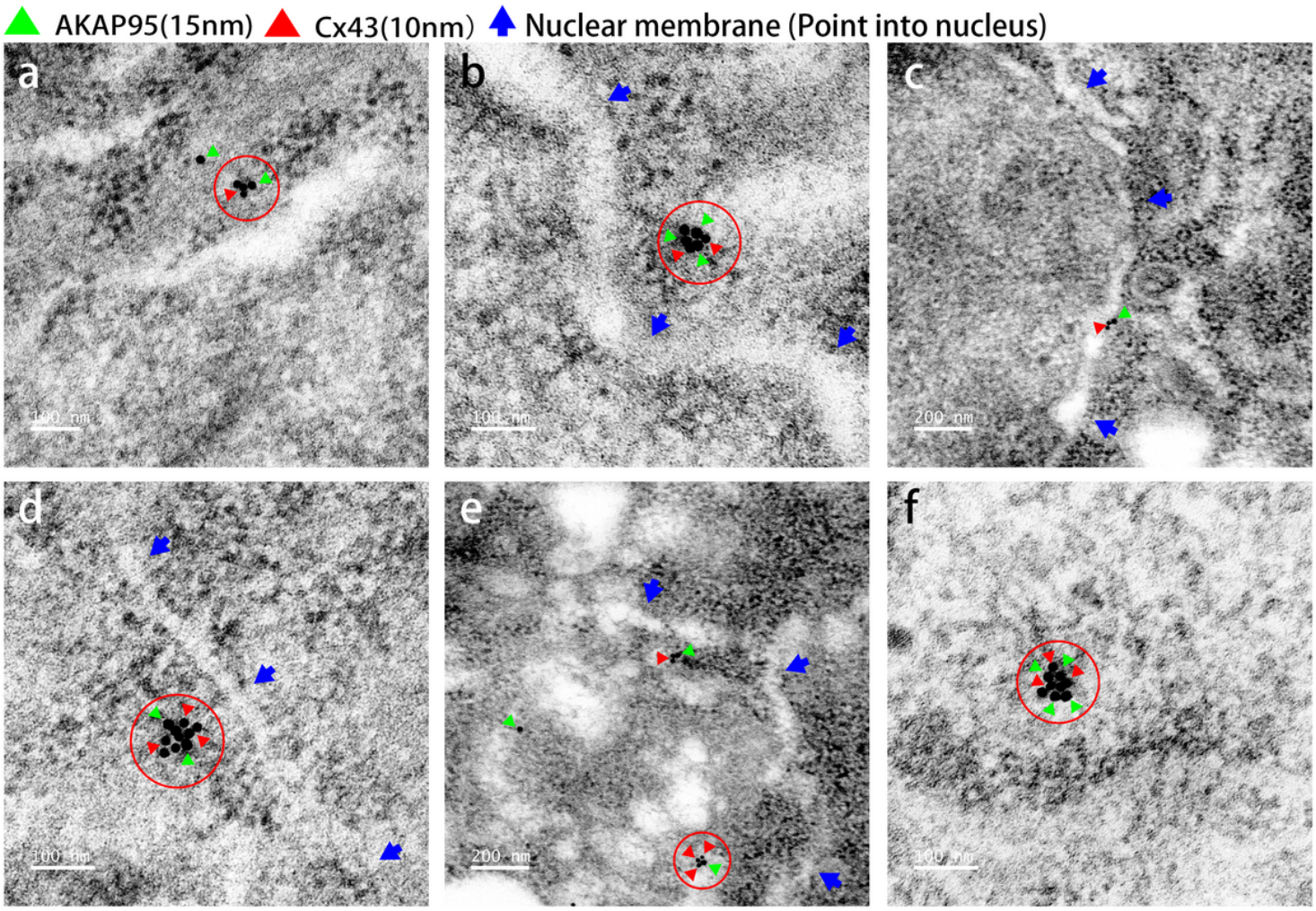

Figure 5

Expression of AKAP95 and Cx43 in arrested cells. (A) FCM was used to detect phases of arrested A549 cells. Cells of control group were treated without drugs. (B)Total proteins were extracted from arrested A549 and Beas-2B cells and detected by WB. Gray value of GAPDH band was used to normalized data. The ratio of gray value of AKAP95 and Cx43 band to GAPDH band was used as variable for statistical analysis among groups (* means $p<0.05$; **means $p<0.01$).

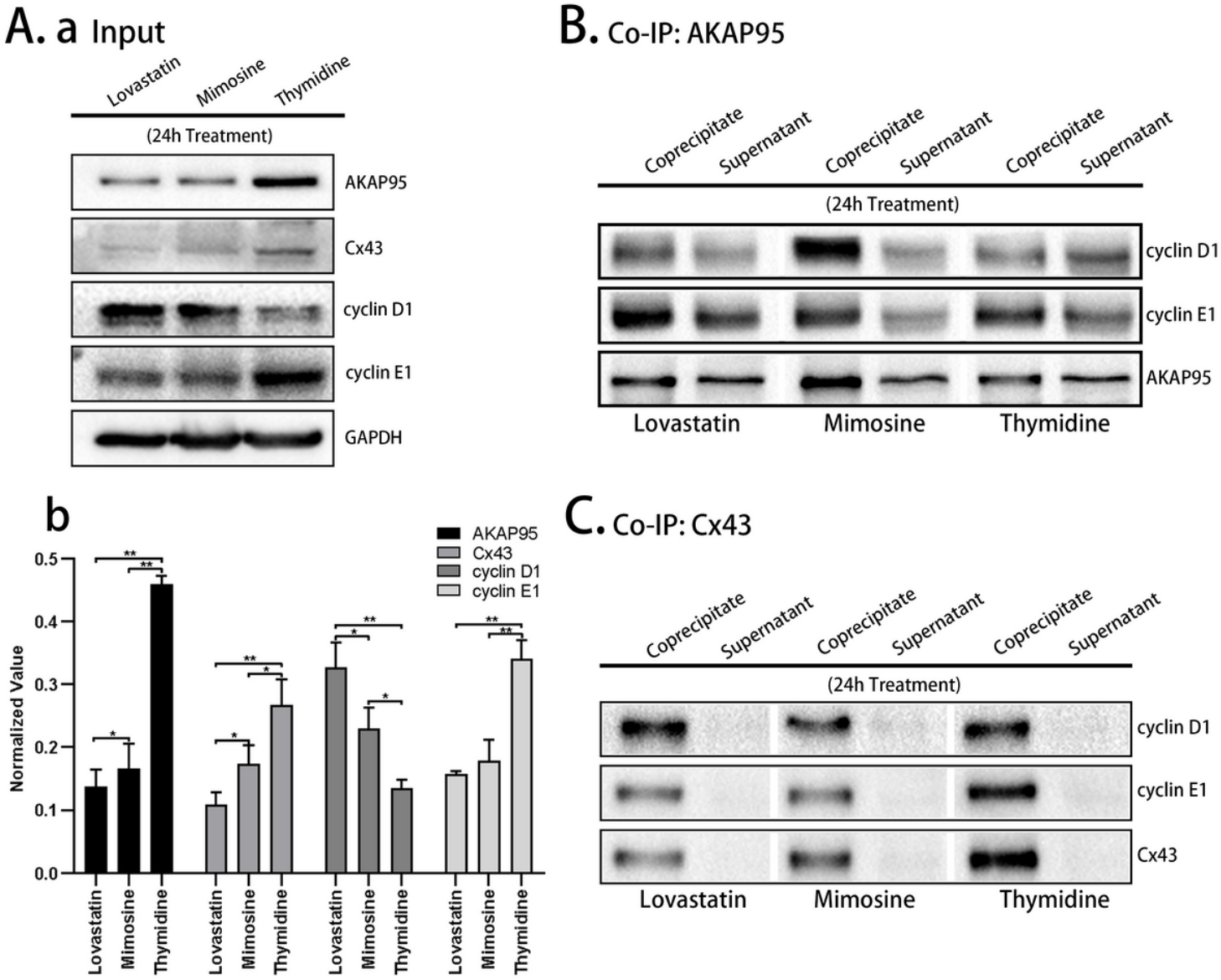

Figure 6

Bindings of AKAP95, Cx43, cyclin D1, and cyclin E1 during G1 phase in A549 cells. (A) a. Expression of AKAP95, Cx43, cyclin D1, and cyclin E1 at P, M, R stages. b. Statistical results of Fig.6Aa. (B) Results of Co-IP: AKAP95 assay of arrested A549 cells. (C) Results of Co-IP: Cx43 assay of arrested A549 cells.

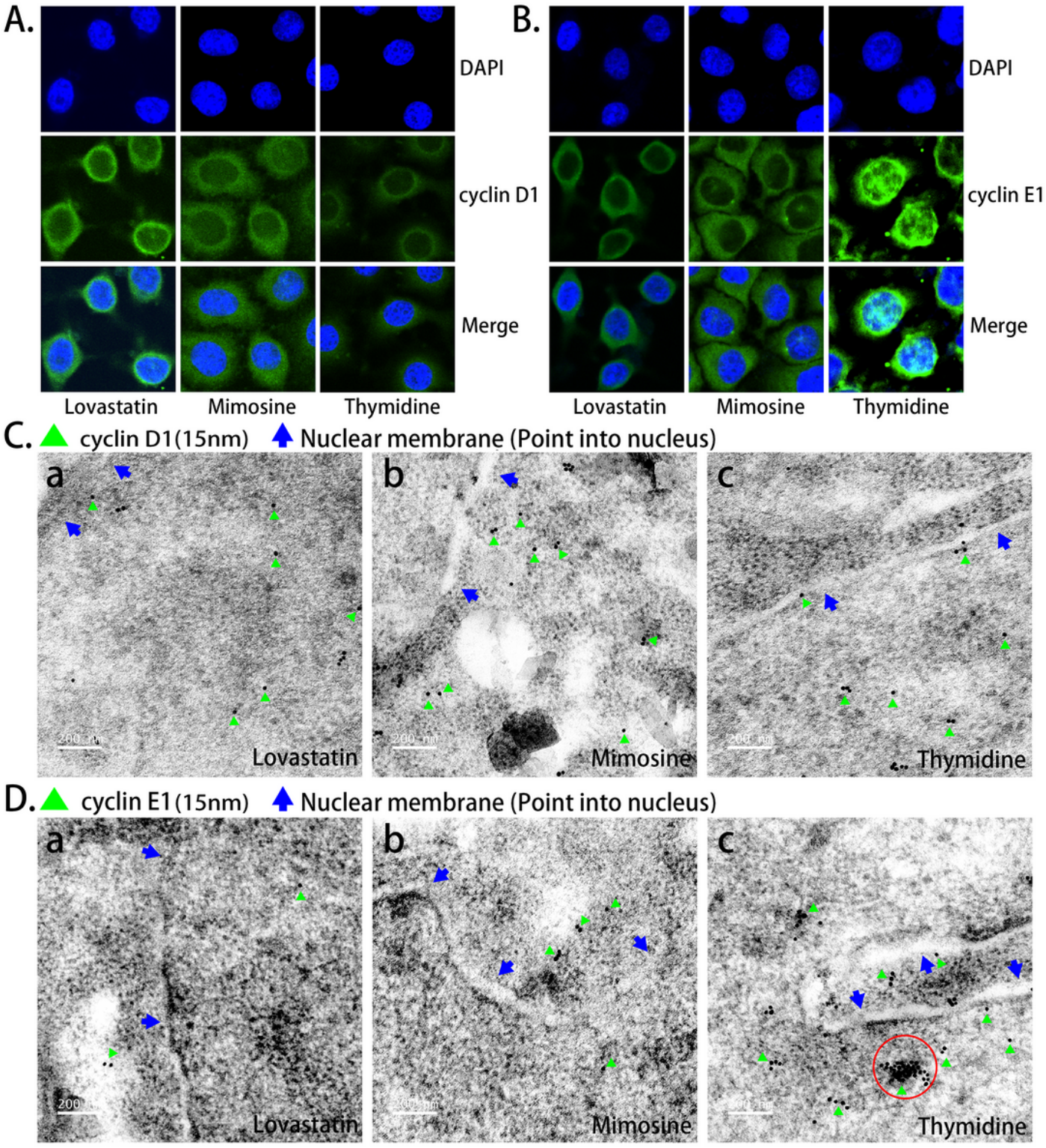

Figure 7

Location of cyclin D1and cyclin E1 in arrested A549 cells. (A) The first row showed DAPI，The second row showed location of cyclin D1，The third row showed merge images of DAPI and cyclin D1. (B). The first row showed DAPI，The second row showed location of cyclin E1，The third row showed merge images of DAPI and cyclin E1. (C) Dilution ratio of Gold labeled IgG was 1:100. Blue arrows pointed into nucleus and the border of strong refraction is nuclear membrane. a., b., c. showed location of cyclin D1 in cells at

different stages respectively. (D) Dilution ratio of Gold labeled IgG was 1:100. Blue arrows pointed into nucleus and the border of strong refraction is nuclear membrane. Protein aggregate of cyclin E1 is marked by red circles. a., b., c. showed location of cyclin E1 in cells at different stages respectively.

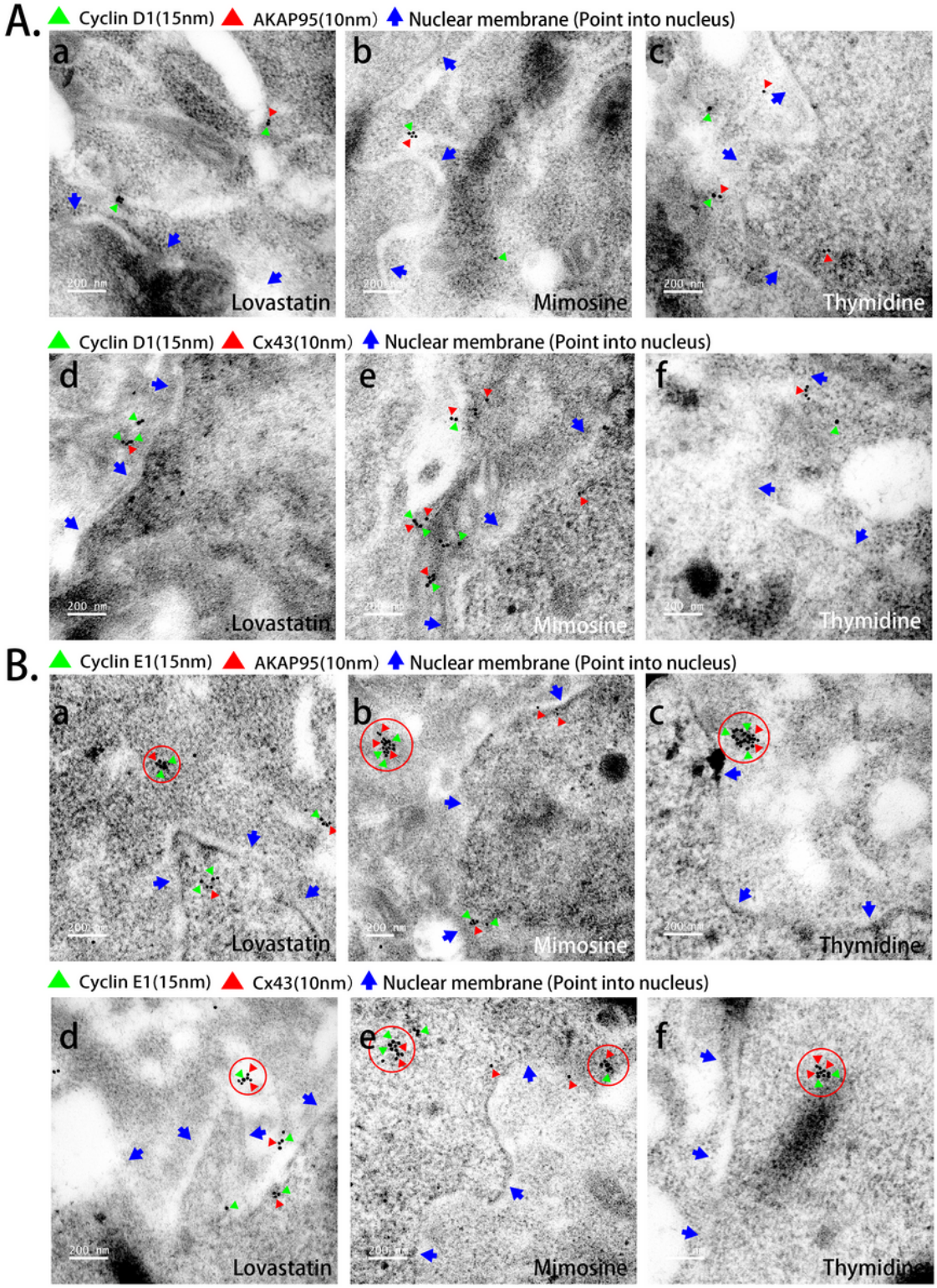

Figure 8

Location of AKAP95/Cx43-cyclin D1 and AKAP95/Cx43-cyclin E1 complex in arrested A549 cells. Dilution ratio of Gold labeled IgG was 1:1000. Blue arrows pointed into nucleus and the border of strong refraction

was nuclear membrane. Protein aggregates were marked by red circles. (A) a., b. &c. AKAP95-cyclin D1 complexes located in cytoplasm. d., e. &f. Cx43-cyclin D1 complexes located in cytoplasm. (B) a., b. &c. AKAP95-cyclin E1 complexes/aggregates located both in cytoplasm and nucleus. d., e. &f. AKAP95-cyclin E1 complexes/aggregates located both in cytoplasm and nucleus.